XX Polish Fluid Mechanics Conference,
Gliwice, 17-20 September 2012

INFLUENCE OF FILTER MEDIA LOADING ON THE FILTRATION EFFICIENCY AND PRESSURE DROP

Rafał PRZEKOP, Arkadiusz MOSKAL
Warsaw University of Technology, Faculty of Chemical and Process Engineering, ul. Waryńskiego 1, 00-645 Warsaw, Poland
E-mail: przekop@ichip.pw.edu.pl

Abstract

Collection of aerosol particles in the particular steps of the technology of their production, and purification of the air at the workplace and atmospheric environment, requires of the efficient method of separation of particulate matter from the carrier gas. There are many papers published last years in which the deposition of particles on fibrous collectors is considered, using classical continuum approach for description of the process. Such an approach is not convenient for studying the influence of particles deposition on the filters performance (filtration efficiency, pressure drop), when one has to introduce nonstaedy-state boundary conditions. The lattice-gas, and lattice-Boltzman methods, which are based on the cellular automata concept, enjoyed rapid development and provided an interesting alternative to traditional numerical techniques for solving the Navier-Stokes equation. Description of particle motion in a fluid requires the knowledge of the velocity field of fluid and particle position at any site of the space and moment of time. For the purpose of this work the lattice-Boltzmann model describes fluid dynamics, while the solid particle motion is modeled by the Brownian Dynamics. Determination of structures of deposited particles on the filter fibre requires the knowledge of a history of the individual particle and its position and velocity vectors. The Lagrangian method of analysis should be used for description of the process. Particle trajectory is calculated for the generalised Besset-Boussinesque-Ossen equation.The aim of this study is to model the influence of filter media loading described by the amount of deposited matters, its spatial distribution and morphology described by porosity and fractal dimension on filter performance.

Key words: lattice-Boltzmann, Brownian Dynamics, multiphase flow

INTRODUCTION

Filtration is one of the effective methods for the removal of particles from an aerosol stream. The development in the formation of specific fibrous structures promises the construction of highly efficient filters for the collection of nanoparticles. A fibrous material operates by capturing an aerosol particle on the fibers within the filter depth, the result being the deposition and re-entrainment of particles approaching the collector. Its effectiveness depends on the particle and fiber size filter porosity, and the material properties of both objects.

The basic principle of deep-bed filtration is the following: first, the solid particles suspended in the fluid are typically smaller than the pores of the filtering medium. As the fluid–solid suspension flows through the filter, the particles present in the suspension deposit at various depths within the bed, that is, on the solid walls bordering the pore spaces. This leads to the progressive clogging of the filter and the subsequent increase of the pressure drop across it. Thus, it is usual to divide the filtration process into two stages: initial and ageing

stages. In the initial stage, the deposition of particles inside the filter is relatively small. Its effect on the properties of the filter is negligible, and the performance of the filter can be regarded as that of the clean filter. On the contrary, the ageing stage corresponds to the clogging of the filter.

There are many papers published recently, in which the deposition of particles on fibrous collectors is considered, using the classical continuum approach for the description of the process (Herzig *et al.*, 1970, Tien, 1989).

Numerous models have been proposed to simulate deep-bed filtration. They can be classified as follows: macroscopic, microscopic, stochastic, and networks. The macroscopic model is formulated for the purpose of describing the overall behavior of deep-bed filtration. In particular, it can predict the histories of the effluent concentration and the pressure drop across the filter. The model consists of the conservation equation of the particles, the assumed filtration rate expression, and the mechanics of the flow through the porous medium.

Whereas the macroscopic approach rather considers the filter as a "black box," the microscopic approach (also called trajectory analysis model) tries to explain the physics of the deposition processes within the filter. In this way, the microscopic approach attempts to quantitatively predict the filter efficiency. The filter is modeled as an assembly of individual collectors of some simple geometry (such as a capillary, a sphere, or a constricted tube). First of all, the flow field associated with the individual collector is obtained either analytically (Tien, 1989, Payatakes *et al.*, 1973) or numerically (Acosta *et al.*, 1989). Then, particle trajectories (around or through an individual collector) are calculated from the force balance that acts on the particle. The individual collector efficiency corresponds to the fraction of particles encountering the collector. Finally, the overall filter efficiency is deduced from the individual collector efficiency by simple association laws.

The continuum assumption of the Navier-Stokes equations is valid provided the mean free path of the molecules is smaller than the characteristic dimensions of the flow domain. If this condition is violated, the fluid will no longer be under local thermodynamic equilibrium and the linear relationship between the shear stress and rate of shear strain (Newton's law of viscosity) cannot be applied. Velocity profiles, boundary wall shear stresses, mass flow rates and pressure differences will then be influenced by non-continuum effects. In addition, the conventional no-slip boundary condition imposed at a solid-fluid interface will begin to break down even before the linear stress-strain relationship becomes invalid. The ratio between the mean free path and the characteristic dimension of the flow geometry, d, is commonly referred to as the Knudsen number, Kn:

$$Kn = \lambda/d \tag{2}$$

The value of the Knudsen number determines the degree of rarefaction of the gas and the validity of the continuum flow assumption. For $Kn < 10^{-2}$, the continuum hypothesis is appropriate and the flow can be described by the Navier-Stokes equations using conventional no-slip boundary conditions. However, for $10^{-2} < Kn < 10^{-1}$ (commonly referred to as the slip-flow regime) rarefaction effects start to influence the flow and the Navier-Stokes equations can only be employed provided tangential slip-velocity boundary conditions are implemented along the walls of the flow domain. Beyond, $Kn = 10^{-1}$ the continuum assumption of the Navier-Stokes equations begin to break down and alternative simulation techniques approaches must be adopted. Finally, for $Kn > 10$, the continuum approach breaks down completely and the regime can then be described as being a free molecular flow. Under such conditions, the mean free path of the molecules is much greater than the characteristic length scale and consequently molecules reflected from a solid surface travel, on average, many lengths scales before colliding with other molecules.

The modeling of two-phase flow processes is an extremely difficult task within the classical hydrodynamics discipline owing, mainly to the inherent free-boundary complication. The lattice-Boltzman methods enjoyed rapid development and provided an interesting alternative to traditional numerical techniques for solving the Navier-Stokes equation (Przekop and Gradoń, 2011, Angelopulos *et al*., 1998)

.

LATTICE-BOLTZMANN

Complete information on the statistical description of a gas at, or near, thermal equilibrium is assumed to be contained in the one-particle phase-space distribution function $f(x, t, \alpha)$ for the atomic constituents of the system. The variables x and t are the space and time coordinates of the atoms and α stands for all other phase-space coordinates e.g. momentum, momentum flux.

For the isolated gas with collisions the Liouville theorem is modified to the form:

$$\partial_t f + u\nabla f = \Omega(f) \tag{1}$$

where $\Omega(f)$ is a function that models the rate of changes of distribution function.

The form of $\Omega(f)$ was proposed by Boltzmann. Since collisions preserve conservation laws, by integration of Boltzmann equation over the continuity equation and momentum tensor equation describing the macrodynamics of the system can be derived. To build the cellular-space picture with a dynamics of the collective motion predicted by Navier-Stokes equation, a lattice on which particles move, a collision rules and other restrictions characteristic for a chosen model should be defined.

Lattice gas methods were pure cellular automaton. Models, using this approach, assume totally discrete physical space, time and the node state. The considered population consists a set of identical particles (each with unit mass, moving with the same average velocity). Particles occupying the same node collide in each time step. Exclusion principle says that there cannot be more than one particle in node, moving in the same direction. The collision rules conserve mass and momentum. After collision, particle moves into the nearest neighbor site on its moving direction. Lattice gas algorithms are very stable and can handle complicated geometry and boundary conditions. The weakness of these methods is that they are “noisy”, requiring spatial and time averaging.

The lattice-Boltzmann model was the next step in developing of such description of the fluid dynamics problems. In a case of the lattice-Boltzmann approach, the node state is described by a continuous function.

The analysis of deposition of aerosol particles and description of the structure of growing agglomerates requires of the knowledge of a fluid motion and particle displacement in a considered region.

The function $f_i(x,t)$ denotes number of fluid particles entering the site x at time t with velocity e_i. Macroscopic quantities such as density ρ or momentum ρu are defined as:

$$\rho = \sum_i f_i, \qquad \rho u = \sum_i f_i e_i \tag{2}$$

The evolution of the system is described by the expression:

$$f_i(x + e_i, t + 1) - f_i(x, t) = \Omega_i(f) \tag{3}$$

where $\Omega_i(f)$ is the collision term.

The outcome of collision can be approximated by assuming that the momentum of interacting particles will be redistributed at some constant rate toward an equilibrium distribution $f_i^{eq}(x, t)$. This simplification is called single-time-relaxation approximation and can be expressed by the equation:

$$\Omega_i = \frac{1}{\tau}(f_i^{eq}(x,t) - f_i(x,t)) \tag{4}$$

In the single-time-relaxation approximation, the momentum distribution at each lattice site is forced toward the equilibrium distribution at each timestep. In the absence of external forces, the equilibrium distribution of a state with zero net momentum is just equal of momentum in each direction. The rate of change toward equilibrium is 1/τ, the inverse of relaxation time, and is chosen to produce the desired value of the fluid viscosity.

$$\nu = \frac{c_s^{\,2}}{2}(2\tau - 1) \tag{5}$$

The equilibrium distribution $f_i^{eq}(x,t)$ is given as follows:

$$f_i^{\,eq} = \rho\alpha_i(1 + \frac{e_i u}{c_s^{\,2}} + \frac{1}{2}(\frac{e_i u}{c_s^{\,2}})^2 - \frac{u^2}{2c_s^{\,2}}) \tag{6}$$

where a_i is model dependent constants and c_s is the sound speed.

When the fluid particle enters the solidified site, it changes its moving direction for the opposite one. This method naturally leads to zero-velocity at the solid level. When we want to introduce the no-slip boundary conditions some assumed part of particles is bounced back, while the rest of the particles are redistributed among other directions.

The equation of state for the discrete space has a form:

$$P = C_s^{\,2}\rho \tag{7}$$

where P is a pressure inside a system.

In traditional (continuum) flow analyses, a no-slip velocity constraint is enforced along all solid-fluid interfaces. The notion behind the no-slip condition arises from the fact that there should be no discontinuities in the velocity field within the fluid as this would give rise to infinite velocity gradients and therefore infinite shear stresses. A similar argument can be employed for conditions at the wall. However, the no-slip constraint is strictly only valid if the fluid adjacent to the surface is in local thermodynamic equilibrium; a condition which requires a very high frequency of molecular collisions with the wall. In practice, the no-slip condition is found to be appropriate provided the Knudsen number, $Kn < 10^{-2}$. If the Knudsen number is increased beyond this value, rarefaction effects start to influence the flow and the molecular collision frequency per unit area becomes too small to ensure thermodynamic equilibrium. Under such conditions, a discontinuity in the tangential velocity will form at any solid-fluid interface.

In continuum regime the bounce-back boundary condition is used on the solid level. This means that when a fluid particle enters the solid site, it changes its moving direction for the opposite one. This method naturally leads to zero-velocity at the solid level.

Our model involves two parameters r, s, representing the probability for a particle to be bounced back and slipped forward, respectively. The boundary kernel takes the form (Succi, 2002):

$$K = \begin{pmatrix} r & 0 & s \\ 0 & r+s & 0 \\ s & 0 & r \end{pmatrix} \tag{8}$$

Obviously, the two parameters are not independent and must be chosen such that $r + s = 1$. Assuming second order slip velocity one can write.

$$u_{wall} = AKn\left|\frac{\partial u_x}{\partial n}\right|_{wall} + BKn^2\left|\frac{\partial^2 u_x}{\partial n^2}\right|_{wall} \tag{9}$$

Knudsen number for lattice is given by $\nu/(c_s d)$. Parameters A and B are given by (Sbragaglia and Succi, 2005):

$$A = \frac{c}{c_s}\frac{1-r}{r} \tag{10}$$

$$B = \frac{c^2}{c_s^{\,2}} \tag{11}$$

Values of r can be estimated from experimental data (Maurer *et. al*, 2003)

BROWNIAN DYNAMICS

Determination of structures of deposited particles on the filter fibre requires the knowledge of a history of the individual particle and its position and velocity vectors. The Lagrangian method of analysis should be used for description of the process. Particle trajectory is calculated for the generalised Besset-Boussinesqu-Ossen equation, which in simplified form is reduced to the expression:

$$m\frac{dv}{dt} = F^{(D)} + F^{(ext)} + F^{(R)} \tag{12}$$

where m is a particle mass and v particle velocity vector.

The drag forces for small, spherical particles satisfying Stokes law can be expressed by:

$$F^{(D)} = \frac{3\pi\mu d_p}{C_s}(u - v) \tag{13}$$

where C_s is Cunnigham factor:

$$C_s = 1 + (\frac{2\lambda}{d_o})[1.257 + 0.400\exp(-0.55 d_p / \lambda)] \tag{14}$$

and λ is the mean free path of the gas molecules.

Foundations of the Brownian Dynamics (BD) were established by Chandrasekhar (1943) for a Stokesian particle in stationary fluid and for a force-free field. In this work extension of BD for the case of moving fluid at presence of the external forces derived by Podgórski (2001a, 2001b) was used. Integration of the equation (12) for the time interval Δt, small enough that the host fluid velocity u_i and external force $F_i^{(ext)}$ may be assumed constant over $(t, t + \Delta t)$, gives the following bivariate normal density probability distribution functions $\varphi_i(\Delta v_i, \Delta L_i)$ that during time interval Δt the particle will change its i^{th} component of velocity by Δv_i and it will be displaced by the distance ΔL_i in i^{th} direction.

$$\varphi_i(\Delta v_i, \Delta L_i) = \frac{1}{2\pi\sigma_{vi}\sigma_{Li}\sqrt{1-\rho^2}} \exp\left\{ -\frac{1}{2(1-\rho)^2}\left[\left(\frac{\Delta v_i - <\Delta v_i>}{\sigma_{Li}} \right)^2 + \right.\right.$$
$$\left.\left. - \frac{2\rho(\Delta v_i - <\Delta v_i>)(\Delta L_i - <\Delta L_i>)}{\sigma_{vi}\sigma_{Li}} + \left(\frac{\Delta L_i - <\Delta L_i>}{\sigma_{Li}} \right)^2 \right] \right\} \tag{15}$$

This distribution may be rearranged to a more convenient form of the product of two Gaussian distributions:

$$\varphi_i(\Delta v_i, \Delta L_i) = \left\{ \frac{1}{\sqrt{2\pi}\sigma_i} \exp\left[-\frac{1}{2}\left(\frac{\Delta v_i - <\Delta v_i>}{\sigma_{vi}} \right)^2 \right] \right\} \times \tag{16}$$
$$\times \left\{ \frac{1}{\sqrt{2\pi(1-\rho^2)}\sigma_{Li}} \exp\left[-\frac{1}{2}\left(\frac{\Delta L_i - <\Delta L_i> - \rho\sigma_{Li}(\Delta v_i - <\Delta v_i>)/\sigma_{vi}}{\sigma_{Li}\sqrt{1-\rho^2}} \right)^2 \right] \right\}$$

The expected values of particle velocity change $<\Delta v_i>$ and the linear displacement $<\Delta L_i>$ are expressed as:

$$<\Delta v_i> = \left[u_i - v_i + F_i^{(ext)}/(m/\tau) \right]\left[1 - \exp(-\Delta t/\tau) \right] \tag{17}$$

$$<\Delta L_i> = \left[u_i + F_i^{(ext)}/(m/\tau) \right]\Delta t - \left[1 - \exp(-\Delta t/\tau) \right]\left[u_i - v_i + F_i^{(ext)}/(m/\tau) \right]\tau \tag{18}$$

where τ is particle relaxation time given by:

$$\tau = \frac{\rho_p {d_p}^2 C_s}{18\mu} \tag{19}$$

The standard deviations σ_{vi}, σ_{Li} are as follows:

$$\sigma_{vi} = \sqrt{(1 - \exp(-2\Delta t/\tau))k_B T/m} \tag{20}$$

$$\sigma_{Li} = \sqrt{(2\Delta t/\tau - 3 + 4\exp(-\Delta t/\tau) - \exp(-2\Delta t/\tau)k_B T/(m/\tau^2)} \tag{21}$$

where k_B is Boltzmann constant and T – absolute temperature.

The coefficient of correlation is given by:

$$\rho = (1 - \exp(-\Delta t/\tau))^2 \left[(1 - \exp(-2\Delta t/\tau))(2\Delta t/\tau - 3 + 4\exp(-\Delta t/\tau) - \exp(-2\Delta t/\tau)) \right]^{-1/2} \tag{22}$$

We can therefore formulate the following generalised algorithm for the Brownian dynamics. For a given initial particle position and its initial velocity components, v_i, at a moment t, we calculate the local fluid velocity, u_i, the external forces, $F_i^{(ext)}$, then, one calculates the expected values $<\Delta v_i>$ and $<\Delta L_i>$ from the equations (17) - (18) and the correction coefficient, ρ, from the equation (22) . Next, we generate two independent random values G_{Li}, G_{vi}, having Gaussian distribution with zero mean and unit variance. Finally we calculate the change of particle velocity, Δv_i, and the particle linear displacement, ΔL_i, during time stem Δt from the expressions accounting for deterministic and stochastic motion:

$$\Delta v_i =< \Delta v_i > + G_{vi}\sigma_{vi} \tag{23}$$

$$\Delta L_i =< \Delta L_i > + \rho G_{vi}\sigma_{Li} + (1-\rho^2)G_{Li}\sigma_{Li} \tag{24}$$

All the steps are repeated for each co-ordinate i = 1, 2, 3. Having determined the increments Δv_i and ΔL_i the new particle velocity at the moment $t + \Delta t$ is obtained as $v_i(t+\Delta t) = v_i+\Delta v_i$, and in the same manner the new particle position is calculated. After completing one time-step of simulations, the next step is performed in the same way.

RESULTS AND DISCUSSION

The aim of this study was to model the time evolution of single and simple systems of fibers efficiency and their morphology described by porosity and fractal dimension. So far the calculations of monodisprese aerosol were perfomed. Figure 1 shows the pictures of dendrite formed by particles of 500 nm diameter on the fiber of diameter 1 μm observed from the upflow. The main direction of gas flow was normal to the axis of the fiber. The superficial air velocity was 0.1 m/s. The time interval between next pictures is 10 seconds. Figures 2-4 show the evolution of dendrite structure for simple systems of the fibers such as two parallel fibers (Fig. 2), two crossed fibers (Fig. 3) and four fibers forming the net (Fig. 4).

As one can see, during the filtration process, more and more particles is deposited on the fiber in the same period of time. Also one can observe that initially slender structures become to be more compact during the filtration process, as the free spaces in dendrite are loaded with depositing particles. These qualitive observations are consistent with data presented on the Fig. 5-9.

The filtration efficiency is initially approximately constant with some fluctuations and after the initial stage of filtrations starts to grow rapidly.

The evolution od pressure drop ΔP for each case (Fig. 6) is shown in comparison to the initial pressure drop on single fiber denoted as ΔP_0.

The quality factor, q_f, which time evolution is presented at Fig. 7 is defined by

$$q_f = -\frac{\ln(1-E)\Delta P_o}{\Delta P} \tag{25}$$

where E is filtration efficiency [(1-E) is called penetration]. The initial increase and later decrease of its value is consistent with experimental data (Davies, 1966)

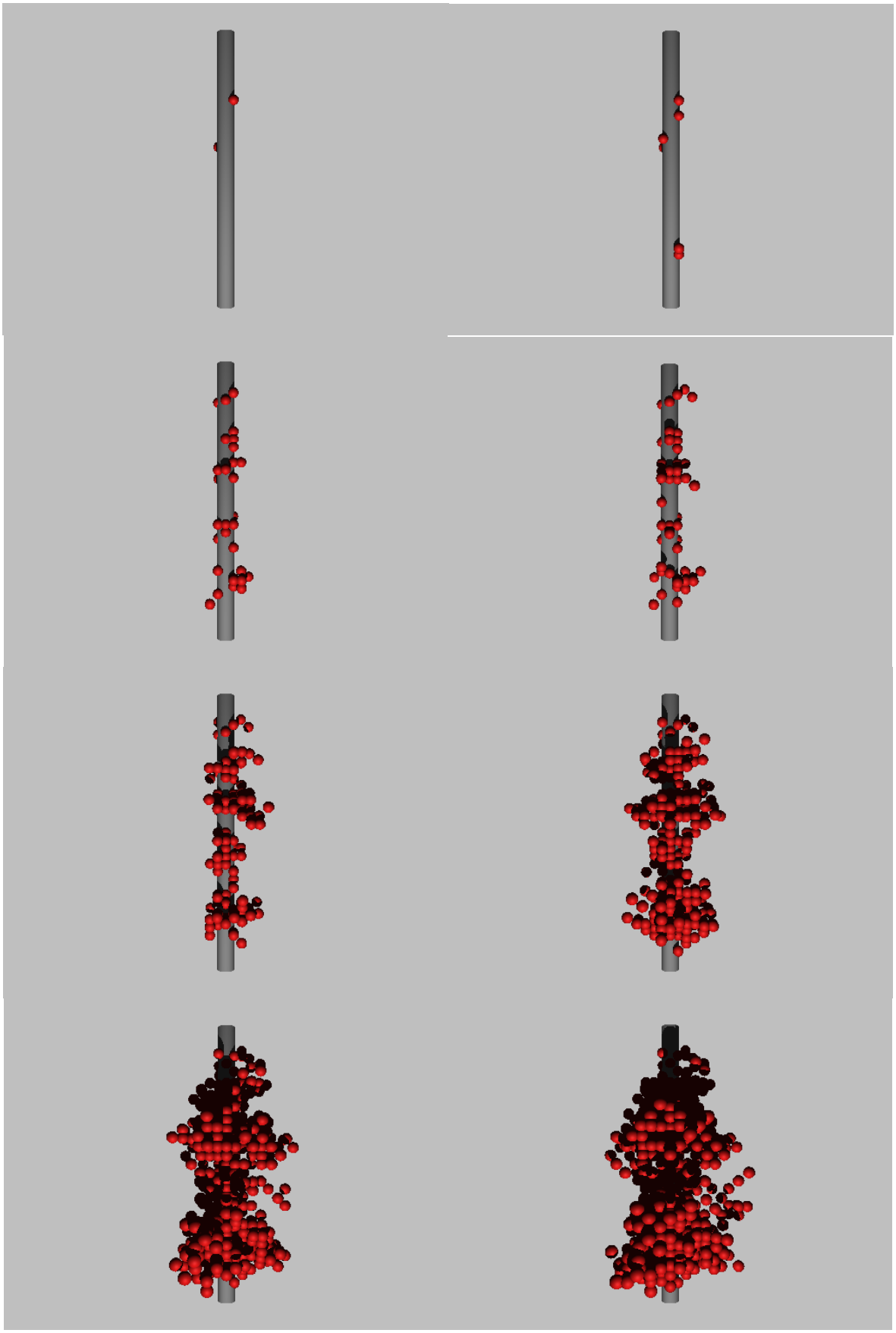

Fig. 1 Stages of dendrite growth (view from the upflow).

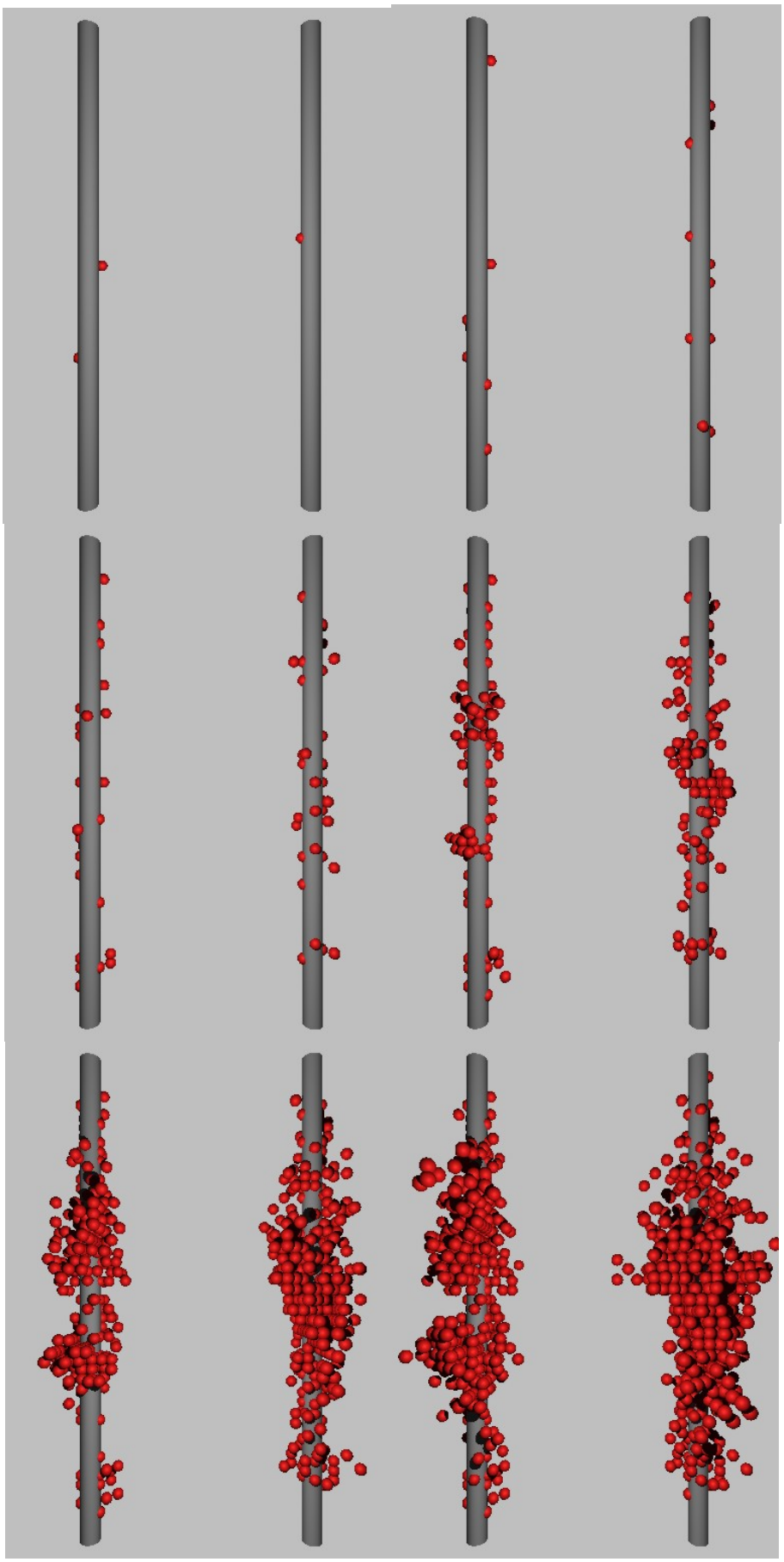

Fig. 2 Stages of dendrite growth (view from the upflow).

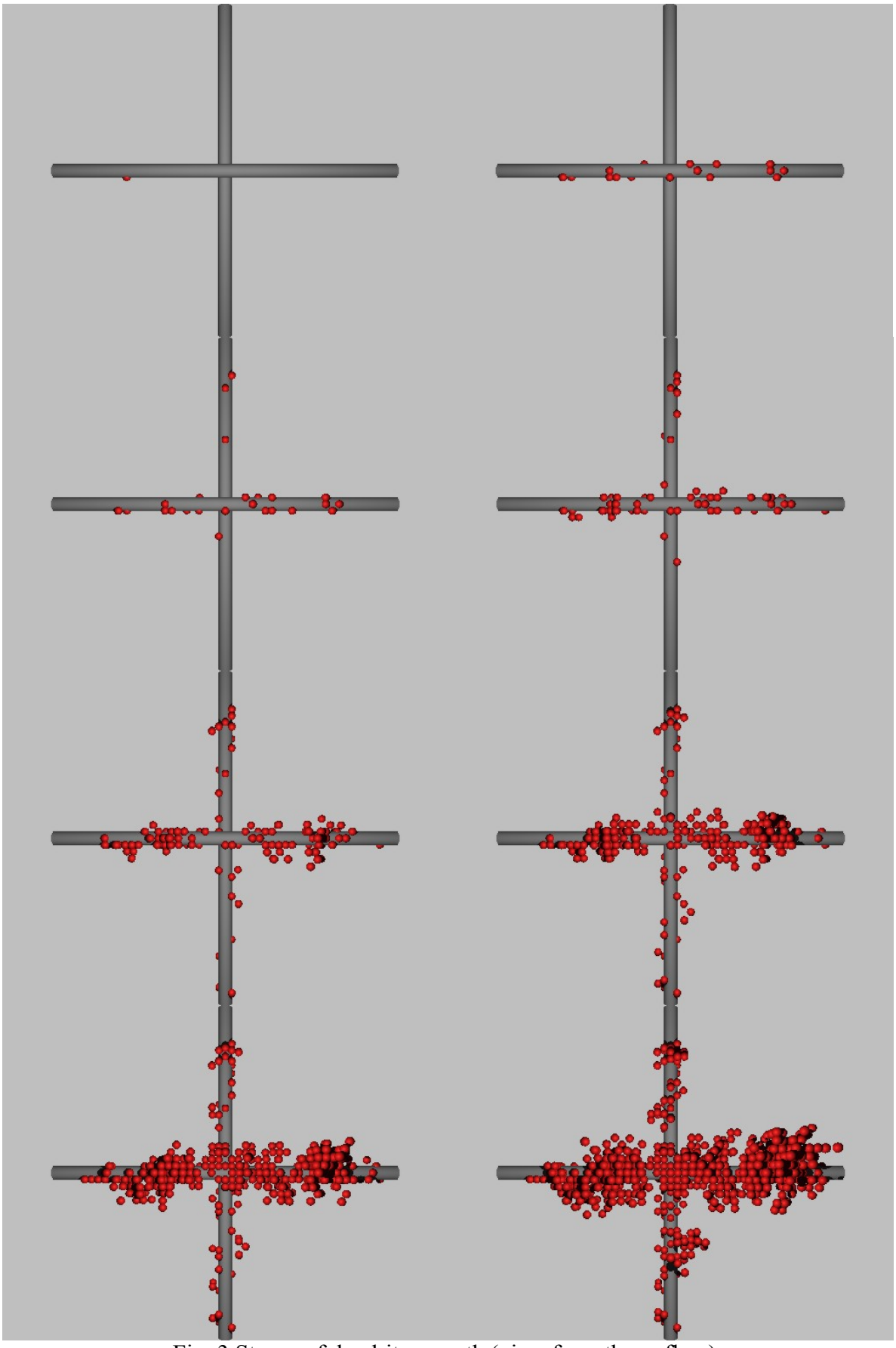

Fig. 3 Stages of dendrite growth (view from the upflow).

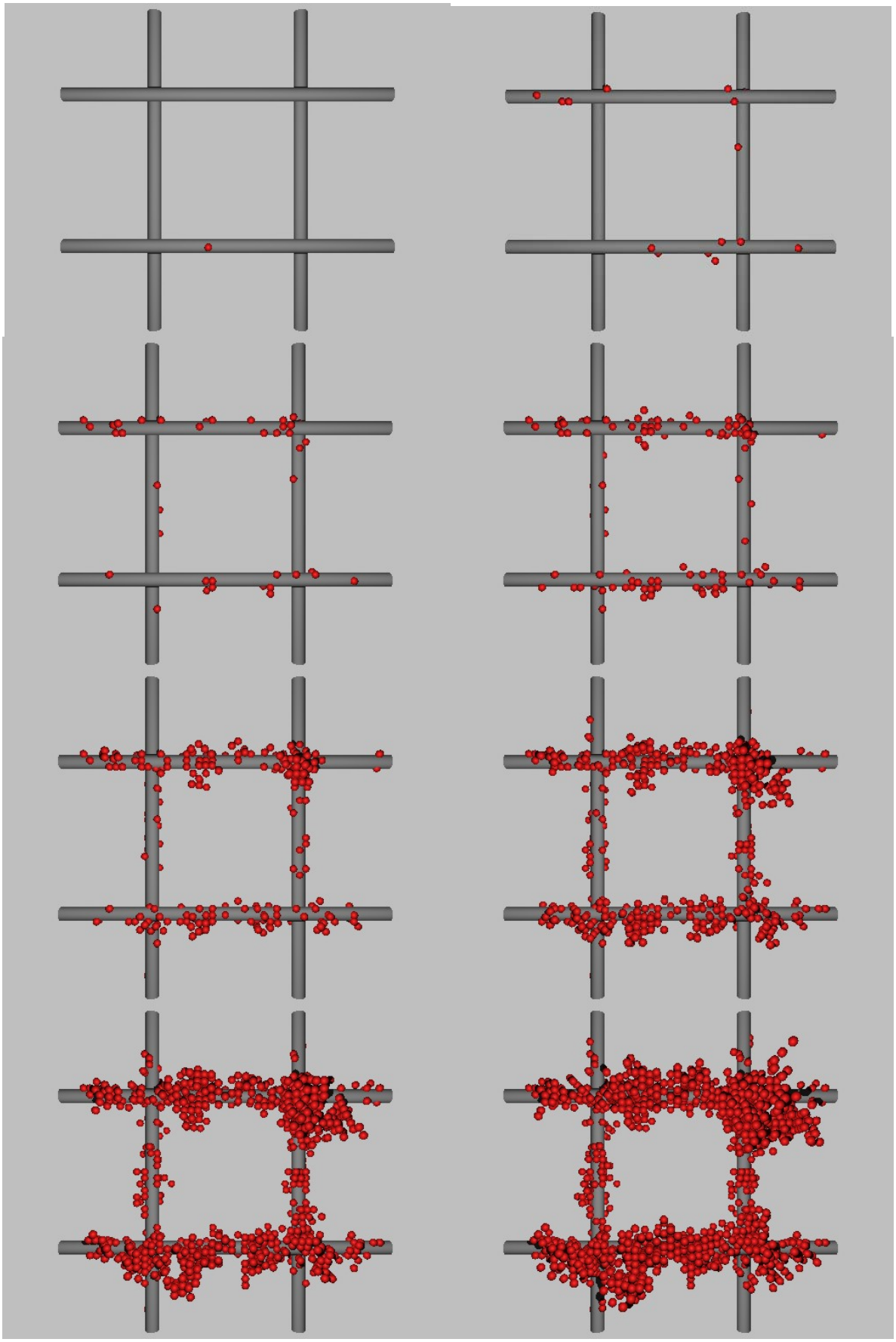

Fig. 4 Stages of dendrite growth (view from the upflow).

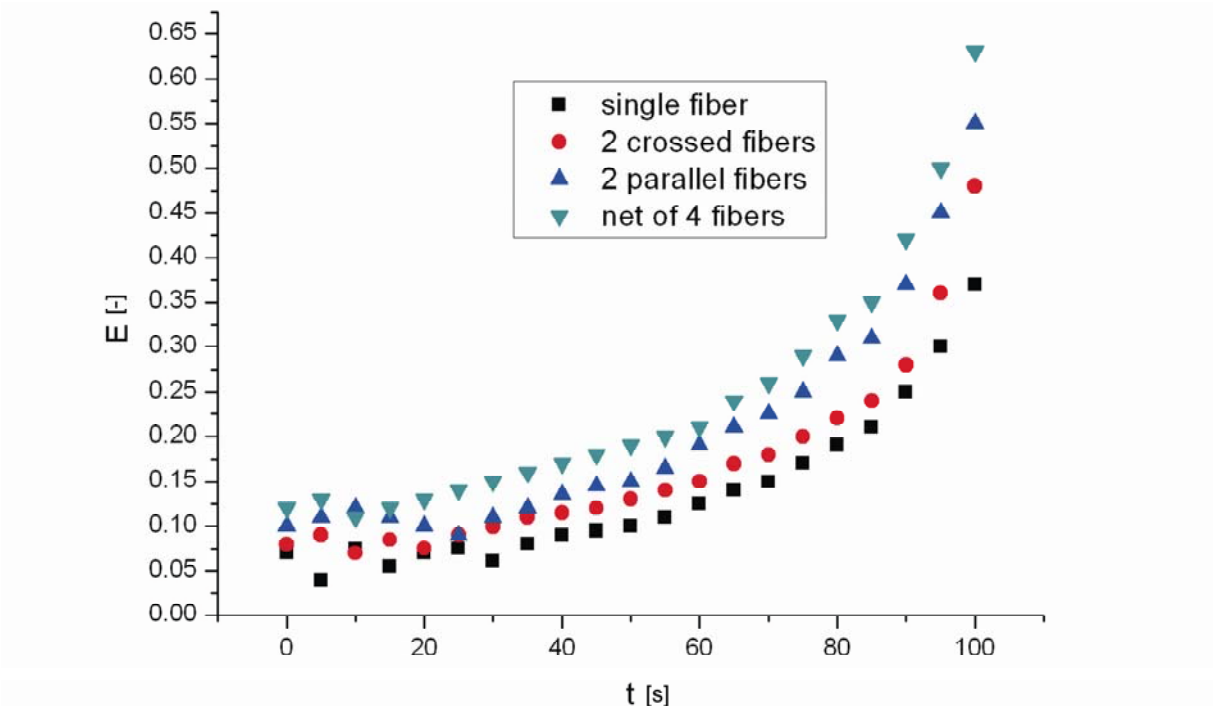

Fig. 5 Time evolution of the system of the fibers efficiency.

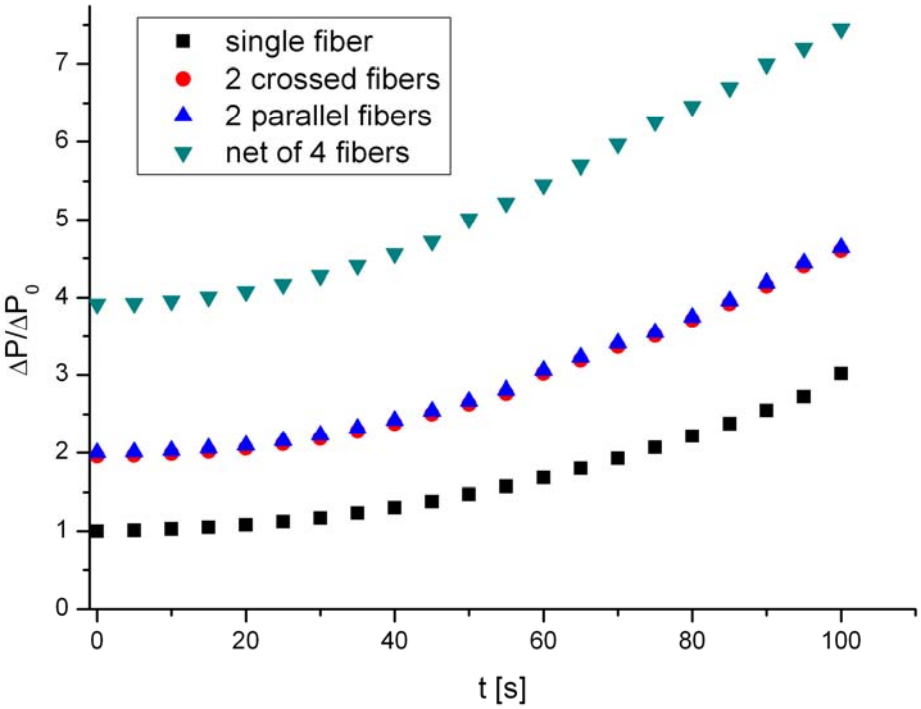

Fig. 6 Time evolution of pressure drop

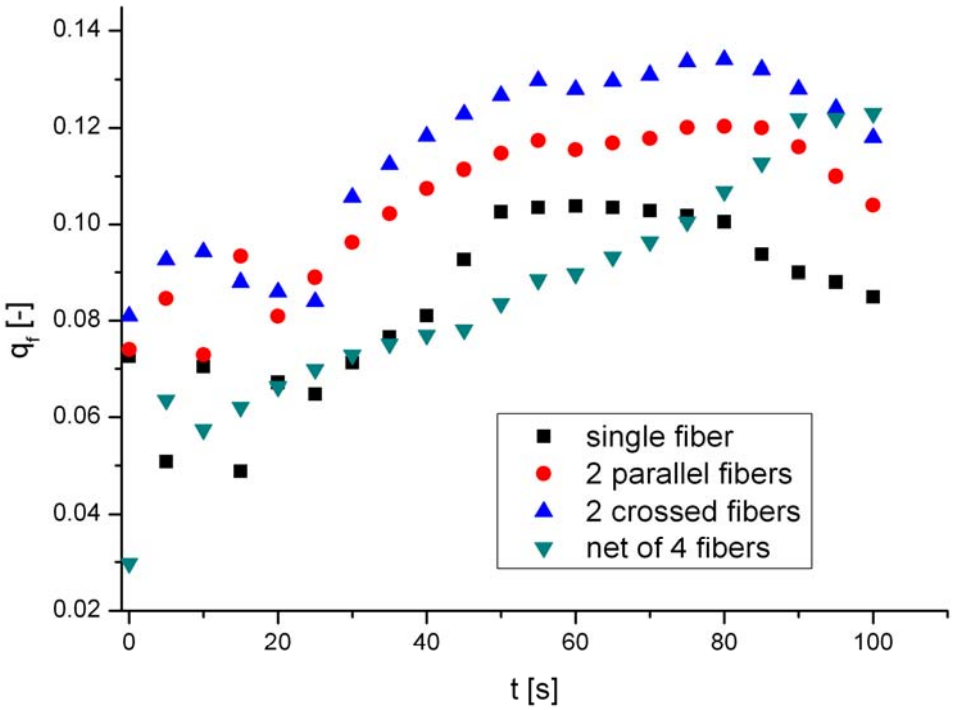

Fig. 7 Time evolution of normalized quality factor

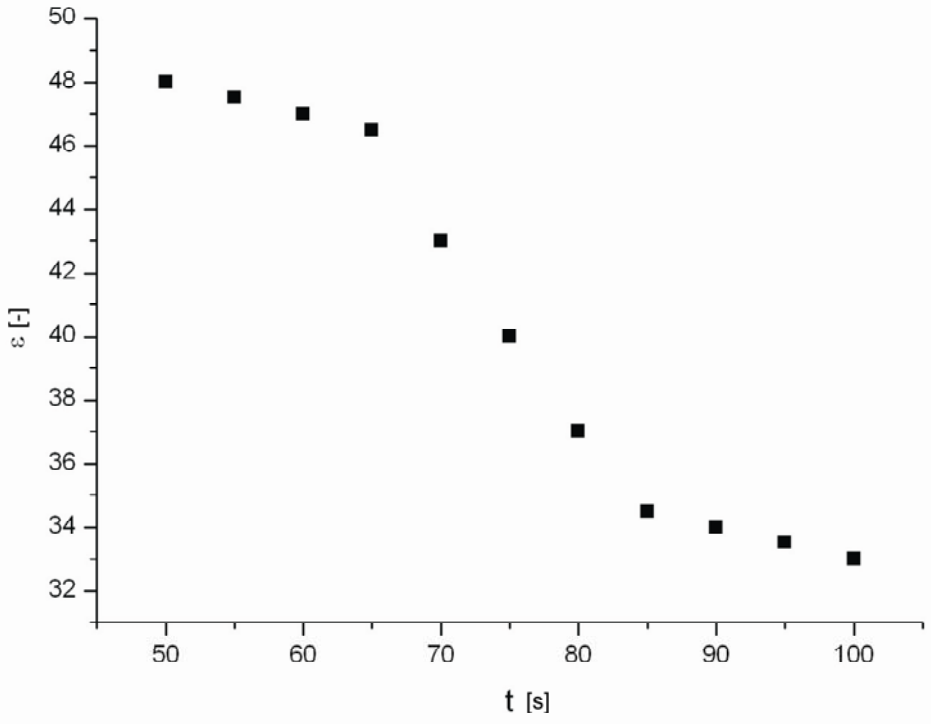

Fig. 8 Time evolution of dendrite porosity.

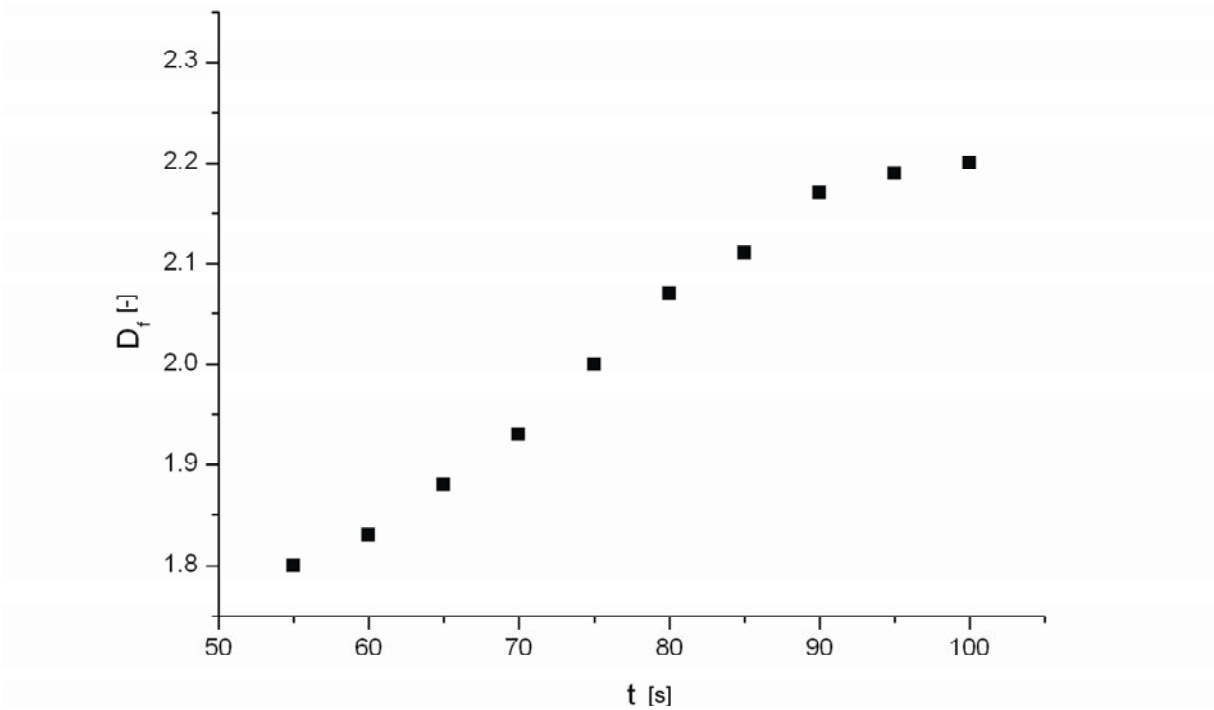

Fig. 9 Time evolution of dendrite fractal dimension.

The increase of dendrites fractal dimension and decrease of their porosity in time can be observed. The fractal dimension, D_f, is calculated as a slope of a line

$$\ln(R_g) = D_f \ln(N) \tag{26}$$

where R_g is radius of gyration and N is number of particles forming the dendrite.

The porosity of dendrite was calculated as follows. The structure was covered by a set of cubes of dimension l_i. The void fraction of deposited structure summarized over all structure defines a step value of the $\varepsilon_i(l_i)$. The dimension of l_i was reduced in the sequence of steps until the calculated value of ε_i reached a stable value

$$\varepsilon = \lim_{li \to l\min} \varepsilon_i \tag{27}$$

One can see that qualitatively the structures of dendrites evolve in the similar way as for single fiber. The efficiency of mentioned above systems is compared with single fiber efficiency in Fig. 5. One can observe that not only fibers packing density, but also their orientation affect the filtration efficiency.

ACKNOWLEDGEMENTS

This work was supported by governmental funding for scientific research in the years 2010-2013 (grant No. N N209 023739).

REFERENCES

Acosta G.F.A., Castillejos E.A.H., Almanza R.J.M., Flores V.A. (1995) *Analysis of liquid flow through ceramic porous media used for molten metal filtration*, Metallurgical and Materials Transactions B*,* Vol. 26B, pp.159-171

Angelopoulos, A., Paunov V.N., Burganos, V.N., Payatakes, A.C. (1998) *Lattice-Boltzmann Simulation of Nonideal Vapor-Liquid Flow in Porous Media*, Physical Review E**,** Vol.57, pp.3237-3245

Chandrasekhar, S. (1943) *Stochastic Problems in Physics and Astronomy*, Reviews of Modern Physics, Vol.15, pp.1-89

Davies, C.N. (1966) *Aerosol Science*, Academic Press, London

Herzig J.P., Leclerc D.M., Le Goff P. (1970) *Flow of suspensions through porous media—Application to deep bed filtration*, Industrial & Engineering Chemistry Research*,* Vol.62, pp.8-35

Maurer, J., Tabeling P., Joseph P., Willamie H. (2003) *Second order slip laws for helium and nitrogen,* Physics of Fluids, Vol.15, pp.2613-2621

Payatakes A.C., Tien C., Turian R.M. (1973) *A new model for granular porous media, I: Model formulation*, AIChE Journal, Vol.19, pp.58-76

Podgórski, A. (2001a) *Brownian Dynamics I. Interpolating functions for drag and resistance forces on a solid spherical aerosol particle moving near a solid wall*, Journal of Aerosol Science, Vol.32 (Suppl. 1), pp.S711-S712

Podgórski, A. (2001b) *Brownian Dynamics II. Algorithms for stochastic simulations of a solid spherical aerosol particle motion near a solid wall*, Journal of Aerosol Science, Vol.32 (Suppl. 1), pp. S713-S714

Przekop, R., Gradoń, L. (2011) *Non-steady-state aerosol filtration in nanostructured fibrous media,* Philosophical Transactions of The Royal Society A: Mathematical, Physical and Engineering Sciences, Vol.369, pp.2476-2484

Sbragaglia M., Succi S. (2005) *Analytical calculation of slip flow in lattic-Boltzmann models with kinetic boundary conditions,* Physics of Fluids, Vol.17, art. no. 093602

Succi, S. (2002) *Mesoscopic modeling of slip motion at solid-fluid interfaces with heterogeneous catalysis*, Physical Review Letters, Vol. 87, art. no. 96105

Tien C. (1989) *Granular Filtration of Aerosols and Hydrosol*. Boston, MA Butterworths/ Reed Publishing.